Free Radical Biology and Medicine 141 (2019) 475–482

Contents lists available at ScienceDirect

Free Radical Biology and Medicine

journal homepage: www.elsevier.com/locate/freeradbiomed

Original article

Serum electrolytes can promote hydroxyl radical-initiated biomolecular damage from inflammation

Yukako Komaki[a,1], Adam M-A. Simpson[b,1], Jong Kwon Choe[c,1], Margaux M. Pinney[d], Daniel Herschlag[d], Yi-Hsueh Chuang[b], William A. Mitch[b,*]

[a] Graduate Division of Nutritional and Environmental Sciences, University of Shizuoka, Shizuoka, 422-8526, Japan
[b] Department of Civil and Environmental Engineering, Stanford University, 473 Via Ortega, Stanford, CA, 94305, USA
[c] Department of Civil and Environmental Engineering and Institute of Construction and Environmental Engineering, Seoul National University, 1 Gwanak-ro Gwanak-gu, Seoul, 08826, Republic of Korea
[d] Department of Biochemistry, Stanford University, Stanford, CA, 94305, USA

ARTICLE INFO

Keywords:
Chronic inflammatory disorders
Reactive oxygen species
Carbonate radical
Protein degradation

ABSTRACT

Chronic inflammatory disorders are associated with biomolecular damage attributed partly to reactions with Reactive Oxygen Species (ROS), particularly hydroxyl radicals (˙OH). However, the impacts of serum electrolytes on ROS-associated damage has received little attention. We demonstrate that the conversion of ˙OH to carbonate and halogen radicals via reactions with serum-relevant carbonate and halide concentrations fundamentally alters the targeting of amino acids and loss of enzymatic activity in catalase, albumin and carbonic anhydrase, three important blood proteins. Chemical kinetic modeling indicated that carbonate and halogen radical concentrations should exceed ˙OH concentrations by 6 and 2 orders of magnitude, respectively. Steady-state γ-radiolysis experiments demonstrated that serum-level carbonates and halides increased tyrosine, tryptophan and enzymatic activity losses in catalase up to 6-fold. These outcomes were specific to carbonates and halides, not general ionic strength effects. Serum carbonates and halides increased the degradation of tyrosines and methionines in albumin, and increased the degradation of histidines while decreasing enzymatic activity loss in carbonic anhydrase. Serum electrolytes increased the degradation of tyrosines, tryptophans and enzymatic activity in the model enzyme, ketosteroid isomerase, predominantly due to carbonate radical reactions. Treatment of a mutant ketosteroid isomerase indicated that preferential targeting of the active site tyrosine accounted for half of the total tyrosine loss. The results suggest that carbonate and halogen radicals may be more significant than ˙OH as drivers for protein degradation in serum. Accounting for the selective targeting of biomolecules by these daughter radicals is important for developing a mechanistic understanding of the consequences of oxidative stress.

1. Introduction

Chronic inflammatory disorders [1], including atherosclerosis [2], arthritis [3], and several neurodegenerative diseases [4], are associated with damage to biomolecules (e.g., proteins) resulting from Reactive Oxygen Species (ROS), chlorine, and proteases emitted by leukocytes [1–7]. ROS include superoxide ($O_2^{\bullet-}$), hydrogen peroxide (H_2O_2), and hydroxyl radical (˙OH), although subsequent interactions produce Reactive Nitrogen Species (e.g., peroxynitrite) and chlorine [2]. High ROS levels are associated with oxidative stress, including damage to proteins [1–7]. Because ˙OH is far more reactive than $O_2^{\bullet-}$ and H_2O_2, ˙OH is believed to play an important role in damaging biomolecules [1–3,6,7], but demonstrating the contribution of specific ROS is difficult.

ROS-associated biomolecular damage could result from intracellular ROS production by mitochondria or from ROS emitted to serum by leukocytes [1–3] or glial cells [4]. The impact of serum electrolytes on ROS reactivity with biomolecules has received little attention. Here, we demonstrate that ˙OH reactions with the high levels of carbonates and halides typical of serum can fundamentally alter the degradation of amino acids in proteins and enhance the loss of enzymatic activity. Accounting for serum electrolytes is critical for developing a fundamental understanding of inflammation-associated damage by ROS.

Hydroxyl radical reactions with carbonates and halides produce carbonate radical ($CO_3^{\bullet-}$) and Reactive Halogen Species (RHS; e.g.,

* Corresponding author.
E-mail address: wamitch@stanford.edu (W.A. Mitch).
[1] These authors contributed equally to this work.

https://doi.org/10.1016/j.freeradbiomed.2019.07.023
Received 23 May 2019; Received in revised form 11 July 2019; Accepted 22 July 2019
Available online 23 July 2019
0891-5849/

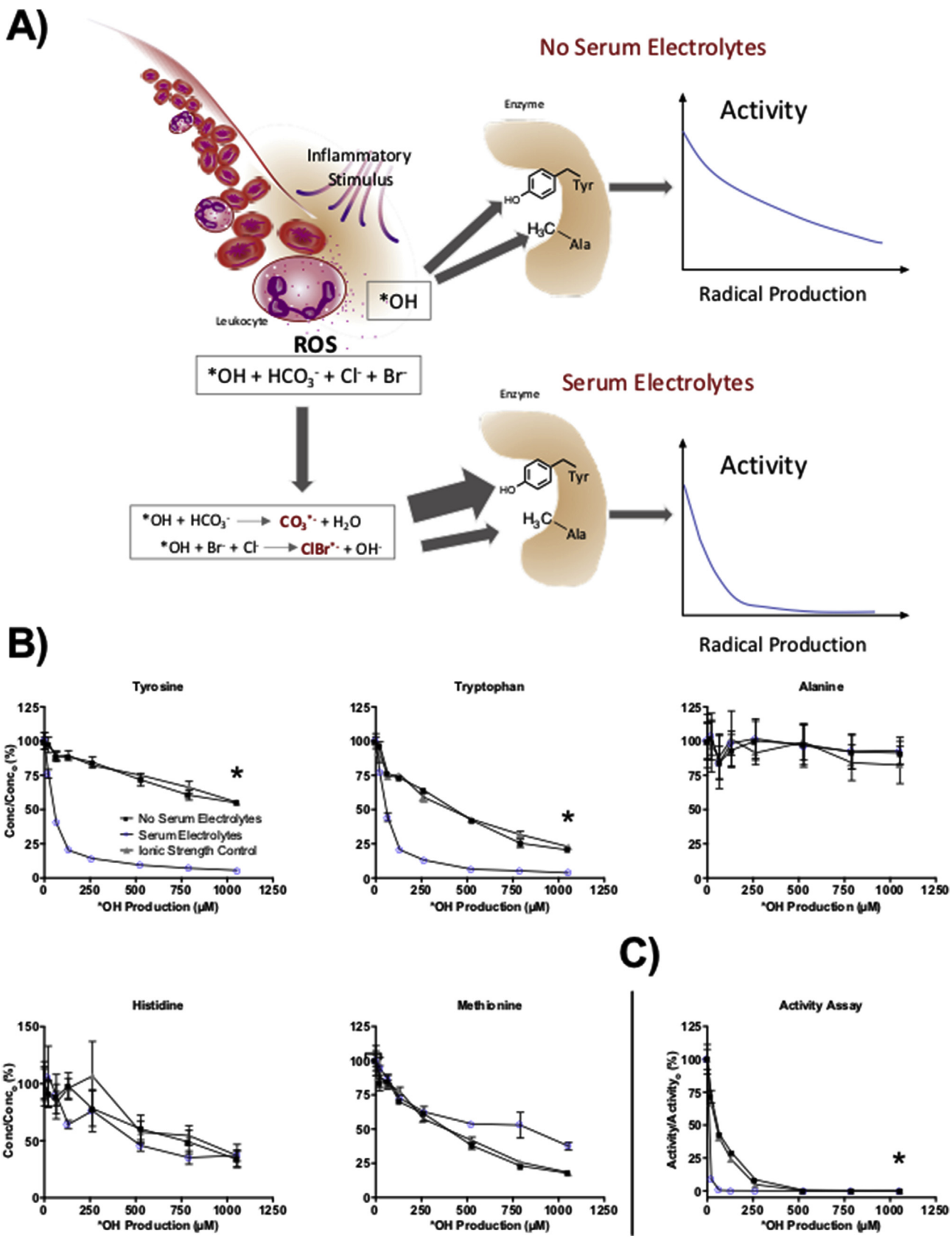

Fig. 1. Serum electrolytes promote tyrosine, tryptophan and activity losses in catalase. (**A**) Scheme depicting $^{\bullet}$OH generation by leukocytes following an inflammatory stimulus. $^{\bullet}$OH conversion to daughter radicals favors the selective degradation of tyrosine over alanine and enhances loss of activity. (**B**) Amino acid degradation and (**C**) activity loss during degradation of 0.5 μM catalase vs. cumulative $^{\bullet}$OH produced using γ-radiolysis at pH 7.4 with or without serum electrolytes (100 mM NaCl, 60 μM NaBr, 20 mM $NaHCO_3$) in 10 mM phosphate buffer or in a 57 mM phosphate ionic strength control. Error bars represent the standard error of triplicate experiments. Asterisk (*) indicates difference in AUC between with and without serum electrolytes is ≥ 25% with ≤25% standard error difference.

$^{\bullet}OH + Br^{-} + Cl^{-} \rightarrow ClBr^{\bullet-} + OH^{-}$). Rate constants for amino acid reactions with these daughter radicals vary by orders of magnitude (for $CO_3^{\bullet-}$, $< 10^3\ M^{-1}\ s^{-1}$ for alanine and $4.5 \times 10^7\ M^{-1}\ s^{-1}$ for tyrosine) while those for $^{\bullet}OH$ reactions approach the diffusion limit ($4.3 \times 10^8\ M^{-1}\ s^{-1}$ for alanine and $1.3 \times 10^{10}\ M^{-1}\ s^{-1}$ for tyrosine) [8,9]. While $^{\bullet}OH$ would target amino acids approximately equally, its conversion to these daughter radicals focuses their oxidizing power on the more reactive amino acids, thereby increasing their observed degradation rates (Fig. 1A).

Previous studies have demonstrated that, relative to $^{\bullet}OH$, $CO_3^{\bullet-}$ can selectively degrade methionine, tryptophan and tyrosine within polypeptides [10,11] or alter protein degradation pathways (e.g., promote lysozyme dimerization) [11]. However, these studies generated $CO_3^{\bullet-}$ under conditions clearly favoring $CO_3^{\bullet-}$ over $^{\bullet}OH$ (e.g., reaction of $^{\bullet}OH$ with 700 mM carbonates at pH 10) [10]. The importance to protein degradation of $CO_3^{\bullet-}$ and RHS generated from $^{\bullet}OH$ under serum-relevant conditions was unclear. Davies et al. demonstrated increased tryptophan losses in bovine serum albumin during γ-radiolysis in the presence of 100 mM carbonate at pH 7 [6]. An elegant γ-radiolysis study by Wolcott et al. demonstrated that synthetic solutions containing chloride (150 mM) and carbonate (100 mM) concentrations relevant to the leukocyte phagosome increased bacterial inactivation, due to the generation from $^{\bullet}OH$ of long-lived oxidants, particularly $CO_3^{\bullet-}$ [12]. While $^{\bullet}OH$ dominated the oxidation of dissolved fluorescein (an oxidation probe), reactions of longer-lived oxidants dominated for particle-bound fluorescein [12]. These results suggested that short-lived $^{\bullet}OH$ would dominate the oxidation of proteins dissolved in serum, but protein sequestration in bacteria or tissue cell membranes could restrict reactivity to oxidants with sufficient lifetimes to permit transport to the particle-bound target. We demonstrate the importance of these daughter oxidants for selective targeting of amino acids and loss of enzymatic activity even for aqueous proteins under serum conditions.

2. Materials and methods

2.1. Chemical reagents

Hydrogen peroxide (30% solution), ammonium formate (≥99%, Optima™ LC/MS grade) and 6-aminoquinoline-*N*-hydroxy-succinimidyl ester (AQC) were purchased from Fisher Scientific (Waltham, MA, USA). L-Tyrosine (99.5%) was purchased from Chem Service Inc. Tryptamine (98%), γ-aminobutyric acid (≥99%), sodium phosphate monobasic dihydrate (99%), and sodium phosphate dibasic (99%) were purchased from Sigma-Aldrich (St. Louis, MO, USA). *N*-Acetylated amino acids included: Sigma-Aldrich (St. Louis, MO, USA) *N*-acetyl-L-alanine (~99%), *N*-acetyl-L-aspartic acid (99%), *N*-acetyl-L-cysteine (99%), *N*-acetyl-L-glutamic acid (99%), *N*-acetyl-L-glycine (99%), *N*-acetyl-L-methionine (98.5%), *N*-acetyl-L-phenylalanine (99%), *N*-acetyl-DL-serine (reagent grade), *N*-acetyl-L-tryptophan (99%), and *N*-acetyl-L-tyrosine (99%); Thermo Fisher Scientific Inc. (Ward Hill, MA, USA) *N*-acetyl-L-proline (99%), and *N*-acetyl-L-isoleucine (98%); TCI Co. (Portland, OR, USA) *N*-acetyl-L-leucine (> 99%), and *N*-acetyl-L-valine (> 98%); Santa Cruz Biotechnology Inc. (Dallas, TX, USA) *N*-acetyl-L-asparagine (reagent grade), and *N*-acetyl-L-threonine (reagent grade); Acros Organics (New Jersey, USA) *N*-acetyl-L-glutamine (97%), and *N*-acetyl-L-histidine (99%); Chem-Impex International, Inc. (Wood Dale, IL, USA) *N*-acetyl-L-lysine (> 99%); MP Biomedicals, Inc. (Solon, OH, USA) *N*-acetyl-L-arginine (99%). 5(10)-Estrene-3,17-dione for KSI activity measurements was purchased from Steraloids. Milli-Q water (electrical resistivity > 18.0 MΩ-cm; Milli-Q purification system; Millipore) was used in all experiments unless otherwise noted.

2.2. Model proteins

Lyophilized albumin from human serum (≥97%), lyophilized catalase from bovine liver (2000–5000 units/mg protein), and lyophilized carbonic anhydrase from bovine erythrocytes (≥95%, specific activity; ≥3500 W-A units/mg protein) were purchased from Sigma-Aldrich. For ketosteroid isomerase (KSI) expression, QuikChange (Stratagene, La Jolla, CA) site-directed mutagenesis was used to incorporate the Y32F/Y57F/Y119F mutations into the KSI gene encoded on a pET-21c plasmid. Mutations were confirmed by sequencing miniprep DNA from DH5α cells on an ABI3730xl capillary sequencer (Elim Biopharmaceuticals). The wild-type (WT) and Y32F/Y57F/Y119F constructs were expressed in *E. coli* BL21(DE3) cells and purified as previously described [13]. Table S1 summarizes details for each protein.

2.3. Gamma irradiation

Proteins were dissolved in solutions of either 1) 10 mM phosphate buffer at pH 7.4 (no serum electrolytes - control), 2) 10 mM phosphate buffer at pH 7.4 amended with 100 mM NaCl, 60 μM NaBr and 20 mM $NaHCO_3$ (serum electrolytes), or 3) 10 mM phosphate buffer at pH 7.4 amended with 10.5 mM NaH_2PO_4 and 36.5 mM Na_2HPO_4 (i.e., 57 mM total phosphate) as an ionic strength control. Each solution was purged with N_2O gas for > 30 min to reach saturation. Then the solution was aliquoted into a 2-mL clear-glass vials and the vials were sealed headspace-free with Teflon-lined septa. Sample vials were exposed to γ radiation at room temperature within a Mark I model 25 irradiator (JL Shepherd and Associates, San Fernando, CA) with a ^{137}Cs source. The production of hydroxyl radical by γ-radiolysis is detailed in Chuang et al. [14]. Briefly, γ-radiolysis of water produces $^{\bullet}OH$ and other species as primary products (equation (1)) [15], where the coefficients provide primary product yields (i.e., G values in μmol J^{-1}). The N_2O rapidly converts hydrated electron (e_{aq}^{-}) and hydrogen atom to $^{\bullet}OH$ (equations (2) and (3)). Fricke dosimetry was used to calibrate the dose received by the samples (7.2 Gy/min) [15]. The dose of 7.2 Gy/min yields a steady-state $^{\bullet}OH$ production rate of 4.4 μM/min. *N*-Acetyl amino acid and protein solutions were analyzed after various exposure times ranging up to 6 h, corresponding to 2592 Gy or 1584 μM $^{\bullet}OH$. Due to safety concerns, the solutions were not continually purged with N_2O during γ-radiolysis, since the irradiator was not within a fume hood. However, the solubility of N_2O in water at room temperature is 29 mM [16]. Based on the stoichiometry of equation (1), the consumption of N_2O after 6 h of irradiation would be only 0.86 mM.

$$H_2O \xrightarrow{\text{Gamma Ray}} (0.28)^{\bullet}OH + (0.06)^{\bullet}H + (0.27)e_{aq}^{-} + (0.05)H_2 + (0.07)H_2O_2 + (0.27)H^{+} \quad (1)$$

$$N_2O + e_{aq}^{-} \rightarrow N_2 + OH^{-} + {}^{\bullet}OH\ (k = 9.1 \times 10^9\ M^{-1}\ s^{-1}) \quad (2)$$

$$N_2O + {}^{\bullet}H \rightarrow N_2 + {}^{\bullet}OH\ (k = 2.1 \times 10^6\ M^{-1}\ s^{-1}) \quad (3)$$

2.4. Protein digestion and analysis

The protein digestion and analysis procedure was similar to that described in detail previously [17] and is summarized below. Free amino acids were liberated from proteins by acid-catalyzed hydrolysis using methanesulfonic acid. A 0.5 mL aliquot of each γ-irradiated sample was mixed with 0.5 mL of 8 N methanesulfonic acid and 0.2 wt % tryptamine as a scavenger within a crimp-top vial (2 mL) to minimize evaporation. The crimp-top vials were flushed with nitrogen for 30 min and incubated at 110 °C for 24 h, followed by neutralization with an equal amount of 4 N NaOH. After spiking with γ-aminobutyric acid as an internal standard (100 μM final concentration), a 20 μL aliquot of the neutralized sample was mixed with 60 μL borate buffer solution (pH 8.8) and 20 μL of acetonitrile solution containing 10 mM 6-aminoquinoline-*N*-hydroxy-succinimidyl ester (AQC) in a microcentrifuge tube. Mixed samples were then incubated at 55 °C for 10 min. Derivatized amino acids were quantified via liquid chromatography equipped with

triple quadrupole mass spectrometry (Agilent 1260 HPLC system coupled with a 6460 triple quadrupole mass spectrometer) using electrospray ionization in negative mode. Derivatized amino acids were separated on an Agilent Poroshell 120 EC-C18 column (3.0 cm × 50 mm, 2.7 μm) held at 35.0 °C at a flowrate of 0.4 mL/min using 5 mM ammonium formate in Milli-Q water and acetonitrile as the mobile phases. The eluent profile was 95% ammonium formate and 5% acetonitrile for 2 min, a linear gradient to 10% ammonium formate and 90% acetonitrile over 4 min and held for 2 min, a linear gradient back to 95% ammonium formate and 5% acetonitrile over 1 min and held for 5 min. A multiple reaction monitoring (MRM) mode was adopted for selective detection of amino acids and the internal standard as shown in Table S2. Mass spectrometry was operated with the nebulizing gas pressure set to 45 psi. The sheath gas temperature and flow were set to 250 °C and 9 L/min, respectively. The nozzle voltage was 500 V. The mass spectrometer capillary voltage was set to 3.5 kV. The drying gas temperature and flow rate were 300 °C and 7 L/min, respectively.

2.5. N-Acetyl amino acid analysis

Free *N*-acetyl amino acids were dissolved in either 10 mM phosphate buffer at pH 7.4 (no serum electrolytes - control) or 10 mM phosphate buffer at pH 7.4 amended with 100 mM NaCl, 60 μM NaBr and 20 mM $NaHCO_3$ (serum electrolytes) at 50 μM concentration. Each solution was purged with N_2O gas for > 30 min to reach saturation. Further γ-radiolysis procedures were as reported in Section 2.3. *N*-Acetyl amino acids were quantified via liquid chromatography equipped with triple quadrupole mass spectrometry by a modification of the described in Section 2.4. Briefly, *N*-acetyl amino acids were not derivatized and samples were analyzed directly from the irradiation vials. *N*-Acetyl amino acids were separated on an Agilent Poroshell 120 EC-C18 column (3.0 cm × 50 mm, 2.7 μm) held at 35.0 °C at a flowrate of 0.4 mL/min using 0.1% formic acid in Milli-Q water and 10% 10 mM formic acid:90% acetonitrile (organic phase) as the mobile phases. The eluent profile was 98% formic acid and 2% organic phase for 2 min, a linear gradient to 10% formic acid and 90% organic phase over 4 min and held for 1.5 min, a linear gradient back to 98% formic acid and 2% organic phase over 1 min and held for 6.5 min. MRM parameters are reported in Table S2.

2.6. Enzymatic activity determination

The enzymatic activity of catalase was measured by monitoring the disappearance of hydrogen peroxide in 0.05 M phosphate buffer at pH 7.0 spectrophotometrically with an Agilent Cary 60 UV–vis spectrophotometer at 240 nm [18]. The enzymatic activity (units/mg of protein) was calculated based on the linear regression of the change in the absorbance at 240 nm. One Unit corresponds to the decomposition of 1 μmol of H_2O_2 per minute at 25 °C and pH 7.0. For the enzymatic activity of carbonic anhydrase, Wilbur-Anderson Units per mg of protein were quantified by measuring the time required for a CO_2 saturated solution to reduce the pH of 0.012 M Tris-HCl buffer from 8.3 to 6.3 at 0–4 °C [19]. For catalase, the enzymatic activities were quantified in triplicate irradiations of catalase samples, while for carbonic anhydrase, the activities were quantified in duplicate irradiations of carbonic anhydrase samples. The determined enzymatic activity was compared to the non-irradiated sample and plotted as [Activity/Activity$_0$].

The enzymatic activity of KSI was quantified by monitoring the reaction of the enzyme with 1 mM of 5(10)-estrene-3,17-dione at 248 nm with a PerkinElmer Lambda 25 spectrophotometer over 15–20 min [20]. The reaction was conducted in pH 7.2 solution with 4 mM potassium phosphate and 0.1 mM EDTA at room temperature. The turnover number, k_{cat} (sec^{-1}), was determined by fitting the initial rate of activity to the Michaelis-Menten equation with a saturated concentration of the substrate. For each reaction condition, the activity was determined using the average values of at least 2 replicate irradiations of KSI samples. The determined enzymatic activity was compared to the non-irradiated sample and plotted as [Activity/Activity$_0$].

2.7. Michaelis-Menten kinetic constants for KSI

The Michaelis-Menten constants, K_M (μM), for KSI Wild Type and Y32F/Y57F/Y19F were determined by quantifying the initial rate of reaction of the enzymes. For KSI wild type enzymes in serum electrolytes (i.e., 10 mM phosphate buffer at pH 7.4 amended with 100 mM NaCl, 60 μM NaBr and 20 mM $NaHCO_3$), this was conducted at 10 nM enzyme concentration for non-irradiated samples and at 40 nM enzyme concentration after exposure to 66 μM $^{\bullet}OH$. For KSI Y32F/Y57F/Y19F without irradiation or serum electrolytes, this was conducted at 5 nM or 10 nM enzyme concentration. In both cases the substrate ranged from 3.9 to 500 μM 5(10)-estrene-3,17-dione. The activity was determined in the same fashion as explained above for the KSI system. However, the normalized enzymatic velocity (sec^{-1}) was regressed against the corresponding substrate concentration to determine k_{cat} (sec^{-1}) and the half-saturation Michaelis-Menten constant K_M (μM). Fig. S1 provides example results for non-irradiated KSI wild type in the presence of serum electrolytes.

2.8. Kinetic modeling

Kinetic modeling was performed as described previously [14,21] using the computer program Kintecus 4.55 [22]. This model contains 166 elementary reactions obtained from the literature or estimated based upon analogy to similar reactions. These reactions include those involving $^{\bullet}OH$, chloride, bromide, carbonates and their daughter products. The full model with rate constants for each elementary reaction is provided in Yang et al. [23] and Chuang et al. [14]. The model has been validated in previous research for modeling the decay of organic contaminants (e.g., phenol, for which reaction rate constants with many of the radicals are known) in engineered water treatment reactors where $^{\bullet}OH$ was generated by the UV photolysis of hydrogen peroxide [14,23,24], and in seawater where radicals were generated by illumination of natural organic matter with a sunlight simulator [21].

2.9. Statistical analysis

Significant differences between “Serum Electrolytes” and “No Serum Electrolytes” conditions with respect to losses in amino acid concentrations and losses in enzymatic activities relative to their respective non-irradiated controls were evaluated based on the area under the curve (AUC) analysis. Each measure was converted into a percentage of the non-irradiated control measure (e.g., the total tyrosine remaining after a set exposure to $^{\bullet}OH$ relative to the total initial tyrosine as measured in a non-irradiated control). For each plot of percentage remaining amino acid concentration or activity versus cumulative $^{\bullet}OH$ exposure (μM), the AUC was calculated. A *t*-test comparing the AUC for the “Serum Electrolytes” condition and the “No Serum Electrolytes” condition using Bonferroni adjustment to account for all 20 common amino acids was used for the analysis of proteins. A *P*-value < 0.05 demonstrated that the AUC associated with amino acid concentrations or enzymatic activity in the presence of “Serum Electrolytes” and “No Serum Electrolytes” were significantly different. Significant differences were observed for several amino acids in whole proteins or *N*-acetylated amino acids.

As the differences for some of the amino acids were minor, even when statistically significant, we also evaluated more stringent metrics. Whether the degradation of the amino acids or enzymatic activities featured 1) ≥25% difference between the means for the AUC for the serum electrolytes and no serum electrolytes conditions and 2) ≤25% standard error difference for these AUCs was also evaluated. The first condition was selected to indicate that the difference in degradation

behavior of the amino acid or enzymatic activity is important between the serum electrolytes and no serum electrolytes conditions. The second condition was selected to provide an indication of the scatter in the data. These values were calculated based upon the formulae below (equations (4) and (5)), where SE represents the standard error for the AUC calculations for the serum electrolyte ("elect") and no serum electrolyte ("no elect") conditions, and n represents the number of replicates (e.g., n = 4 for the *N*-acetyl amino acid experiments).

$$AUC\ difference = \frac{|AUC_{no\ elect} - AUC_{elec}|}{AUC_{no\ elect}} \quad [4]$$

$$standard\ error\ difference = \frac{\sqrt{\frac{SE^2_{elect}}{n} + \frac{SE^2_{no\ elect}}{n}}}{|AUC_{elect} - AUC_{no\ elect}|} \quad [5]$$

Tables S3, S4 and S5 summarize the results of the AUC analyses. Wherever there was a ≥25% difference in AUC with ≤25% standard error difference between with and without serum electrolytes, this difference was also significant using a *t*-test ($P < 0.05$). Accordingly, the additional AUC criteria were more stringent. For example, the degradation of *N*-acetyl alanine was significantly greater (i.e., lower AUC; $P < 0.05$) in the presence of serum electrolytes (Fig. S3) due to the very low standard error between replicates, but the difference was only 13% (Table S2), suggesting that the difference was unlikely to be important for protein degradation. The degradation of methionine in catalase appeared to be lower in the presence of serum electrolytes (higher AUC), and the difference appeared to be potentially important (26%; Table S4). However, there was high scatter in the data, as indicated by the high standard error difference (39%; Table S4). In the case of *N*-acetyl glycine and several of the other very polar *N*-acetyl amino acids, the high standard error difference frequently was associated with analytical challenges resulting from poor chromatographic separation by HPLC (low chromatographic retention times in Table S2).

3. Results and discussion

3.1. Effect of serum electrolytes on N-acetyl amino acid degradation

A mixture of 50 μM each of the *N*-acetylated analogues of the 20 common amino acids was exposed to $^{\bullet}OH$ generated from water by steady-state γ-radiolysis at pH 7.4 (10 mM phosphate buffer) with or without serum levels of chloride (100 mM), bromide (60 μM) and carbonates (20 mM) [25]. The *N*-acetyl group mimicked the peptide bond. These electrolytes were evaluated because of their high serum concentrations and reaction rate constants with $^{\bullet}OH$ relative to other serum electrolytes [9]. Serum electrolyte concentrations promoted the degradation of *N*-acetylated tyrosine, tryptophan, methionine, histidine, proline and cysteine (i.e., reduced the area under the curve (AUC) by ≥ 25% with ≤25% standard error difference) (Figs. S2–S6 and Table S3). This targeting was similar to that expected from $CO_3^{\bullet-}$ [8,10,11], suggesting the importance of these daughter radicals under serum conditions.

We applied a kinetic model incorporating 166 elementary reactions involving inorganic anions and radicals previously validated for seawater salts [21] to characterize the relative concentrations of $^{\bullet}OH$, $CO_3^{\bullet-}$, and RHS in the presence of serum electrolytes at pH 7.4. This modeling is complicated because $^{\bullet}OH$ generation rates at inflammation sites are unclear, and rate constants for many radical reactions (particularly $CO_3^{\bullet-}$ and RHS) with amino acids and other blood components are unavailable. Considering only inorganic reactions, the model indicates that a steady-state $^{\bullet}OH$ concentration of 10^{-15} M would result in 2.1×10^{-9} M $CO_3^{\bullet-}$ and 1.6×10^{-13} M RHS (predominantly $Br_2^{\bullet-}$ and $ClBr^{\bullet-}$). These concentrations would be modified by reactions with organics in a fashion that is difficult to model, but this modeling suggests the potential significance of $CO_3^{\bullet-}$ and RHS reactions.

3.2. Effect of serum electrolytes on amino acid degradation and activity loss in proteins

We evaluated three important human blood proteins: 1) the enzyme catalase, which degrades H_2O_2 (a ROS), 2) human serum albumin, which constitutes a significant fraction of blood protein [25], and 3) the enzyme carbonic anhydrase, which catalyzes the interconversion of carbon dioxide and bicarbonate to maintain blood pH. Proteins were exposed to $^{\bullet}OH$ generated by steady-state γ-radiolysis at pH 7.4 with or without serum levels of chloride, bromide and carbonates. After treatment, acid digestion liberated amino acids for quantification of residual tyrosine, tryptophan, methionine, histidine and alanine. The first four amino acids were targeted because serum electrolytes increased the degradation of their *N*-acetylated analogues (i.e., decreased the AUC by ≥ 25%) (Table S3), and because they are frequently important components of enzyme active sites (unlike proline). Although serum electrolytes also increased *N*-acetyl cysteine degradation by > 25%, degradation was nearly complete at the lowest $^{\bullet}OH$ exposures with or without serum electrolytes (Fig. S6). Alanine represented other amino acids whose *N*-acetylated analogues were less affected by serum electrolytes.

$CO_3^{\bullet-}$ and RHS react with organic compounds predominantly by one-electron oxidation and H-atom abstraction to produce carbon-centered radicals [26,27], eventually forming various products in aqueous solution, including hydroxylated analogues of the parent amino acids and even dimers (e.g., dityrosine and ditryptophan dimers [1,11]). Because the same products could be formed by one-electron oxidation or H-atom abstraction reactions involving $^{\bullet}OH$ [27], monitoring the production of oxidized amino acid products would not distinguish the importance of $CO_3^{\bullet-}$ and RHS vs. $^{\bullet}OH$. Accordingly, differences in the pattern of parent amino acid degradation in the presence or absence of serum electrolytes were evaluated to indicate the role of $CO_3^{\bullet-}$ and RHS.

For catalase (amino acids for this and other proteins are provided in Table S1), serum-relevant electrolytes were associated with a clear increase in tyrosine and tryptophan degradation (Fig. 1B and Table S4). Catalase enzymatic activity decreased more rapidly than degradation of any particular amino acid; nonetheless, its loss was similarly enhanced by serum electrolytes (Fig. 1C and Table S5). These effects were not observed in 57 mM phosphate, which has an ionic strength equivalent to the serum electrolytes, indicating that these effects result from $^{\bullet}OH$ reactions with specific electrolytes, not an ionic strength effect.

Serum electrolytes also promoted tyrosine loss in human serum albumin, but decreased methionine degradation (Fig. 2 and Table S4). Human serum albumin does not feature enzymatic activity. However, for carbonic anhydrase, serum electrolytes only promoted the loss of histidine but reduced the loss of enzymatic activity (Fig. 3), even though 3 of the 18 histidines (16%) in carbonic anhydrase coordinate a zinc ion in the active site [28]. These results suggest that the electrolyte-promoted degradation of histidines affected histidines outside the active site, potentially due to protection of the active site histidines by their coordination with zinc. The distinct behavior between proteins suggests that differences in the three-dimensional arrangement of amino acids within proteins may affect their susceptibility to oxidation by radicals.

3.3. Probing the targeting of tyrosine by daughter radicals in a model enzyme

Loss of enzymatic function may result from 1) degradation of amino acids in the active site or 2) loss of amino acids elsewhere in the protein whose interactions maintain the overall protein structure needed for adequate function. Serum electrolytes promoted losses of both tyrosines and enzymatic activity in catalase, which features a catalytic tyrosine (Tyr357) [29]. Alternatively, tyrosine, which can form interactions with other residues (e.g., hydrogen bonds), can be important for protein

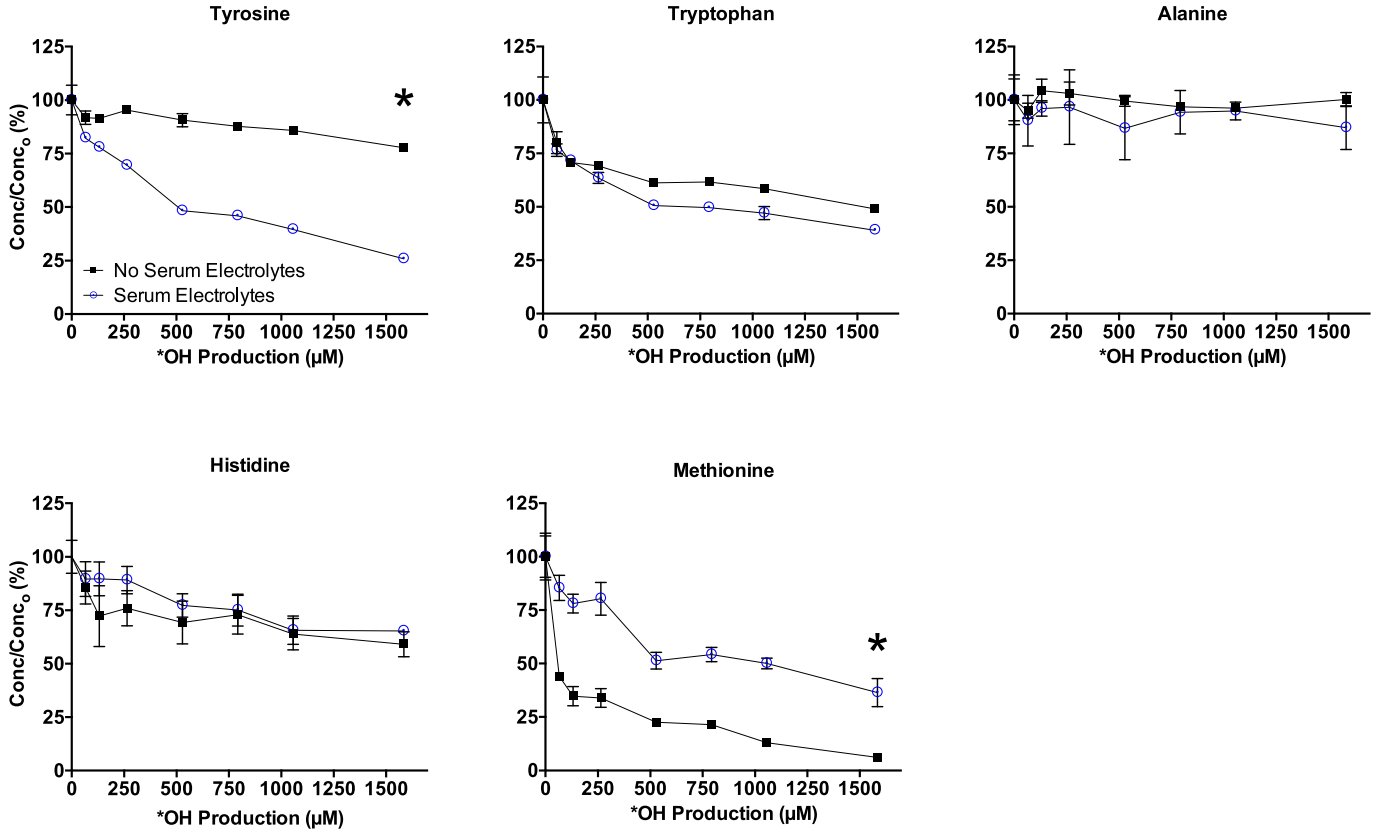

Fig. 2. Serum electrolytes promote tyrosine degradation and inhibit methionine degradation in albumin. Degradation of 5 μM human serum albumin vs. cumulative ˙OH produced using γ-radiolysis at pH 7.4 with or without serum electrolytes (100 mM NaCl, 60 μM NaBr, 20 mM $NaHCO_3$) in 10 mM phosphate buffer. Error bars represent the standard error of triplicate experiments. Asterisk (*) indicates difference in AUC between with and without serum electrolytes is ≥ 25% with ≤25% standard error difference.

stability. When either all tyrosines, methionines, lysines or histidines were replaced in the adenylate kinase enzyme while maintaining its three-dimensional structure and enzymatic function, the greatest reduction in structural stability (measured as protein melting temperature) was observed for the variant in which the tyrosines were replaced [17].

While the protein digestion protocol facilitates quantification of amino acid degradation, the locations of oxidized amino acids within proteins are lost. To examine the importance of tyrosine, we investigated the model enzyme, ketosteroid isomerase (KSI). Compared to catalase (84) and carbonic anhydrase (9), KSI features fewer tyrosines (4), one of which is in the active site and contacts the substrate (Tyr16) [13]. Similar to catalase, serum electrolytes, but not an ionic strength control, increased the losses of tyrosines, tryptophans and enzymatic activity (Fig. 4 and Tables S4 and S5). After exposure to 66 μM ˙OH with serum electrolytes (the maximum exposure for which activity was evaluated), 27% of the four total tyrosines had degraded, and enzymatic activity was reduced by 78% (Table S6). This ˙OH exposure was associated with a 52% reduction in turnover number (k_{cat} declined from 2.7 s^{-1} to 1.3 s^{-1}), and a decrease in affinity (K_M increased from 20 μM to 53 μM) (Table S7). The tyrosine and activity losses after 66 μM ˙OH exposure were the same for 20 mM bicarbonate only and for 20 mM bicarbonate, 100 mM chloride and 60 μM bromide, while the tyrosine and activity losses for only chloride or for only chloride and bromide (i.e., serum electrolytes control without bicarbonate) were indistinguishable from those measured in ionic strength controls (Table S6). These results indicate that $CO_3^{\bullet-}$ was predominantly responsible for the electrolyte-induced enhancement in losses of tyrosine and activity.

If tyrosine degradation focused on the KSI active site tyrosine (Tyr16; 25% of the total tyrosine), its nearly complete degradation might account for the 27% degradation of total tyrosines and the 78% decline in activity after exposure to 66 μM ˙OH with serum electrolytes. To isolate the role of Tyr16, this experiment was repeated with a triple mutant in which the other three tyrosines were replaced by phenylalanines (KSI Y32F/Y57F/Y119F). After exposure to 66 μM ˙OH with serum electrolytes, 45% of Tyr16 was degraded, but the activity loss was 93% (Table S6). These results suggest that degradation of the active site Tyr16 accounted for at most half of the electrolyte-enhanced increase in activity loss. For the wild type KSI, if 66 μM with serum electrolytes also achieved 45% degradation of Tyr16, Tyr16 loss would account for 12% degradation of the total tyrosines, compared to the 27% total tyrosine degradation observed in wild type KSI (Table S6). Accordingly, Tyr16 degradation alone could not account for the entire loss in activity. It is possible that electrolyte-enhanced degradation of tyrosines and other amino acids outside the active site contributed to activity loss if they were important for the structural stability of the active site. Indeed, the triple mutant featured a lower binding affinity (K_M increased from 20 μM to 29 μM) even prior to ˙OH exposure (Table S7). Moreover, conversion of the three tyrosines outside the KSI active site to phenylalanines (i.e., wild type vs. Y32F/Y57F/Y119F KSI) increased the loss of activity after exposure to 66 μM ˙OH from 63% to 79% in an ionic strength control and from 78% to 93% in the presence of serum electrolytes (Table S6).

4. Conclusions

Understanding how amino acid interactions translate into protein structure and function is a complex problem, even without accounting for oxidatively generated modifications to these amino acids. Our results highlight the need for research on oxidative stress associated with

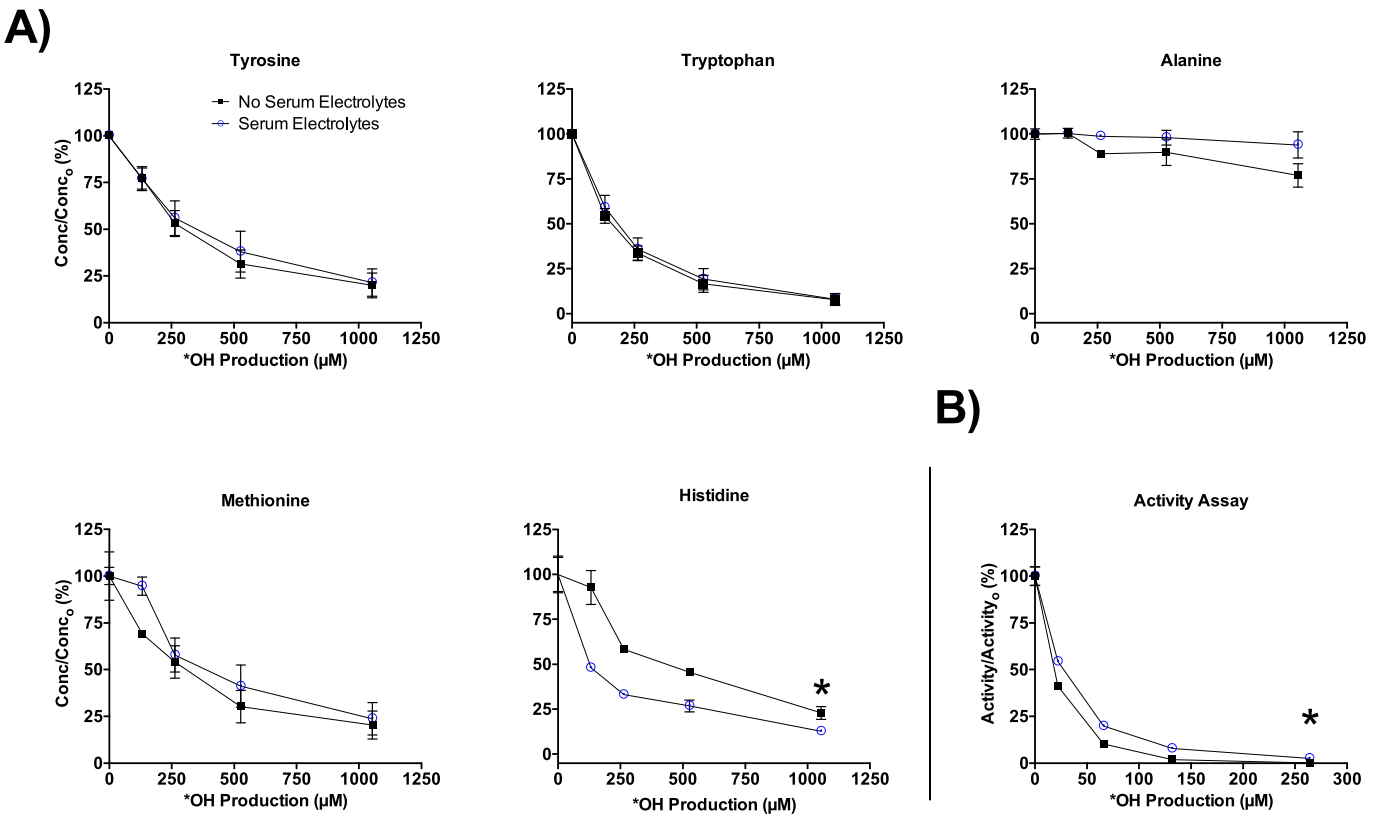

Fig. 3. Serum electrolytes promoted histidine degradation but inhibited activity loss in carbonic anhydrase. Degradation of 3.75 μM carbonic anhydrase vs. cumulative ˙OH produced at 4.4 μM/min using γ-radiolysis at pH 7.4 with or without serum electrolytes (100 mM NaCl, 60 μM NaBr, 20 mM $NaHCO_3$) in 10 mM phosphate buffer. (**A**) Amino acid degradation. (**B**) Activity loss. Error bars represent the range of duplicate experiments. Asterisk (*) indicates difference in AUC between with and without serum electrolytes is ≥ 25% with ≤25% standard error difference.

chronic inflammatory disorders to account for the role of daughter radicals produced from interactions of ˙OH with serum electrolytes. Serum electrolytes altered the degradation of amino acids in all four proteins and of activity in all three enzymes. However, the differences observed between proteins, likely associated with their different three-dimensional structures, suggest the difficulty of defining broadly applicable principles for oxidatively damaged proteins. Regardless, for two of the three enzymes, our findings suggest that serum electrolytes can significantly reduce the ˙OH exposure required to degrade enzymatic activity. These results indicate that serum-derived daughter radicals could be more significant contributors to the biomolecular damage associated with inflammatory disorders than ˙OH.

The scope of this study was limited in several respects. First, this study focusing on highlighting the role of serum electrolytes for ˙OH-mediated protein degradation, rather than the mechanism by which specific proteins degrade. Gamma-radiolysis produced ˙OH uniformly throughout the solution. Iron and other transition metals associated with ˙OH production via Fenton reactions *in vivo* may associate with negatively-charged amino acid moieties (e.g., glutamic acid), leading to selective degradation of neighboring amino acids by ˙OH and its daughter radicals. Thus, differences in the three-dimensional arrangement of amino acids in different proteins could affect the pattern of amino acid degradation. The importance of these differences in protein structure is suggested by the fact that even with the uniform production

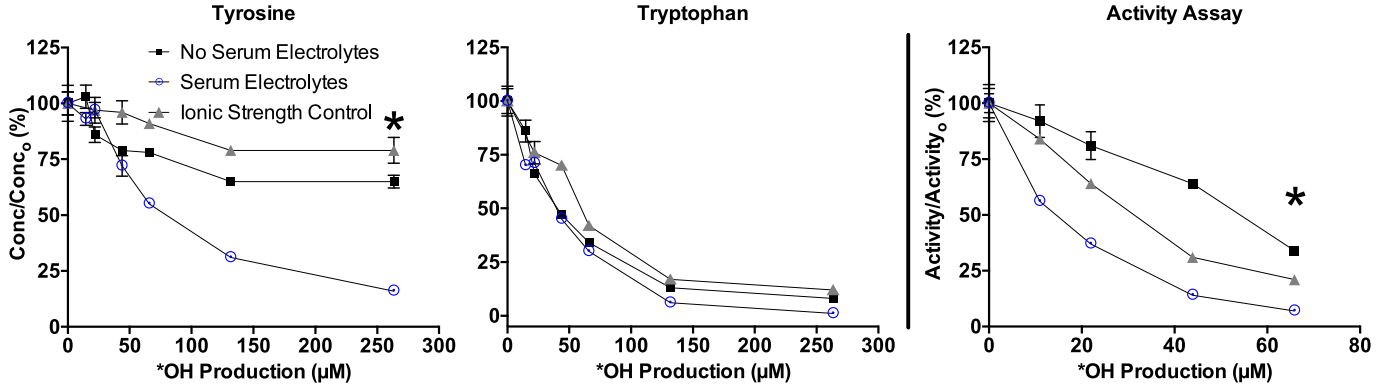

Fig. 4. Serum electrolytes promote tyrosine, tryptophan and activity losses in ketosteroid isomerase (KSI). (**A**) Amino acid and (**B**) activity loss in wild type KSI vs. cumulative ˙OH after treatment of 8 μM KSI using γ-radiolysis at pH 7.4 with or without serum electrolytes (100 mM NaCl, 60 μM NaBr, 20 mM $NaHCO_3$) in 10 mM phosphate buffer or in a 57 mM phosphate ionic strength control. Error bars represent the standard error of replicate experiments (n = 2–5). Asterisk (*) indicates difference in AUC between with and without serum electrolytes is ≥ 25% with ≤25% standard error difference.

of $^{\bullet}OH$ throughout the solutions achieved by γ-radiolysis, we observed differences in the patterns of amino acid degradation between different proteins. Second, $^{\bullet}OH$ is one of many constituents contributing to biomolecular damage during inflammation. The carbon-centered radicals formed via one-electron oxidation or H-atom abstraction from amino acids during their reactions with $^{\bullet}OH$, $CO_3^{\bullet-}$, and RHS [26,27] could react with dissolved oxygen to form peroxy radicals. Purging solutions with N_2O in preparation for γ-radiolysis strips these solutions of dissolved oxygen, preventing the formation of peroxy radicals. Thus, this study did not encompass the contributions to protein degradation of peroxy radicals or other reagents associated with inflammation, including reactive nitrogen species, chlorine and the activity of proteases [2]. Nonetheless, this study indicates the need for research to consider the potential contributions of serum electrolyte-derived daughter radicals to biomolecular damage associated with $^{\bullet}OH$ during inflammatory disorders.

Declarations of interest

None.

Acknowledgements

We thank the members of the Mitch and Herschlag labs for sharing protocols and scientific discussions. Y.K. was supported by the Japan Society for the Promotion of Science Overseas Research Fellowships. A.S. was supported by a Stanford Graduate Fellowship. J.C. was partially supported by the Creative-Pioneering Researchers Program at Seoul National University. M.M.P. was supported by an NSF Graduate Research Fellowship and KSI work was supported by NSF Grant MCB-1714723.

Appendix A. Supplementary data

Supplementary data to this article can be found online at https://doi.org/10.1016/j.freeradbiomed.2019.07.023.

References

[1] M. Mittal, M.R. Siddiqui, K. Tran, S.P. Reddy, A.B. Malik, Reactive oxygen species in inflammation and tissue injury, Antioxidants Redox Signal. 20 (2013) 1126–1167.
[2] R. Stocker, J.F. Keaney, Role of oxidative modifications in atherosclerosis, Physiol. Rev. 84 (2004) 1381–1478.
[3] J.M. McCord, Free Radicals and Inflammation: protection of synovial fluid by superoxide dismutase, Science 185 (1974) 529–531.
[4] J.K. Andersen, Oxidative stress in neurodegeneration: cause or consequence? Nat. Med. 10 (2004) (2004) S18.
[5] E. Kolaczkowska, P. Kubes, Neutrophil recruitment and function in health and inflammation, Nat. Rev. Immunol. 13 (2013) 159.
[6] K.J.A. Davies, M.E. Delsignore, S.W. Lin, Protein damage and degradation by oxygen radicals, J. Biol. Chem. 262 (1987) 9902–9907.
[7] J.K. Hurst, What really happens in the neutrophil phagosome? Free Radic. Biol. Med. 53 (2012) 508–520.
[8] S. Chen, M.Z. Hoffman, Rate constants for the reaction of carbonate radical with compounds of biochemical interest in neutral aqueous solution, Radiat. Res. 56 (1973) 40–47.
[9] G.V. Buxton, C.L. Greenstock, W.P. Helman, A.B. Ross, Critical review of rate constants for reactions of hydrated electrons, hydrogen atoms and hydroxyl radicals ($^{\bullet}OH/^{\bullet}O^-$) in aqueous solution, J. Phys. Chem. Ref. Data 17 (1988) 513–886.
[10] M.M. Zhang, D.L. Rempel, M.L. Gross, A fast photochemical oxidation of proteins (FPOP) platform for free-radical reactions: the carbon radical anion with peptides and proteins, Free Radic. Biol. Med. 131 (2019) 126–132.
[11] V. Paviani, R.F. Queiroz, E.F. Marques, P. Di Mascio, O. Augusto, Production of lysoozyme and lysozyme-superoxide dismutase dimers bound by a ditryptophan cross-link in carbonate radical-treated lysozyme, Free Radic. Biol. Med. 89 (2015) 72–82.
[12] R.G. Wolcott, B.S. Franks, D.M. Hannum, J.K. Hurst, Bactericidal potency of hydroxyl radical in physiological environments, J. Biol. Chem. 269 (1994) (1994) 9721–9728.
[13] D.A. Kraut, P.A. Sigala, B. Pybus, C.W. Liu, D. Ringe, G.A. Petsko, D. Herschlag, Testing electrostatic complementarity in enzyme catalysis: hydrogen bonding in the ketosteroid isomerase oxyanion hole, PLoS Biol. 4 (2006) 501–519.
[14] Y.-H. Chuang, K.M. Parker, W.A. Mitch, Development of predictive models for the degradation of halogenated disinfection byproducts during the UV/H_2O_2 advanced oxidation process, Environ. Sci. Technol. 50 (2016) 11209–11217.
[15] J.W.T. Spinks, R.J. Woods, An Introduction to Radiation Chemistry, third ed., Wiley-Interscience, New Jersey), 1990.
[16] H. Kierzkowska-Pawlak, R. Zarzycki, Solubility of carbon dioxide and nitrous oxide in water + methyl diethanolamine and ethanol + methyldiethanolamine solutions, J. Chem. Eng. Data 47 (2002) 1506–1509.
[17] J.K. Choe, D.H. Richards, C.J. Wilson, W.A. Mitch, Degradation of amino acids and structure in model proteins and bacteriophage MS2 by chlorine, bromine, and ozone, Environ. Sci. Technol. 49 (2015) 13331–13339.
[18] R.F. Beers, I.W. Sizer, A spectrophotometric method for measuring the breakdown of hydrogen peroxide by catalase, J. Biol. Chem. 195 (1952) 133–140.
[19] K.M. Wilbur, N.G. Anderson, Electrometric and colorimetric determination of carbonic anhydrase, J. Biol. Chem. 176 (1948) 147–154.
[20] J.P. Schwans, D.A. Kraut, D. Herschlag, Determining the catalytic role of remote substrate binding interactions in ketosteroid isomerase, Proc. Natl. Acad. Sci. U.S.A. 106 (2009) 14271–14275.
[21] K.M. Parker, W.A. Mitch, Halogen radicals contribute to photooxidation in coastal and estuarine waters, Proc. Natl. Acad. Sci. U.S.A. 113 (2016) 5868–5873.
[22] J.C. Ianni, Kintecus, Windows Version 4.55, (2012) www.kintecus.com.
[23] Y. Yang, J.J. Pignatello, J. Ma, W.A. Mitch, Comparison of halide impacts on the efficiency of contaminant degradation by sulfate and hydroxyl radical-based advanced oxidation processes (AOPs), Environ. Sci. Technol. 48 (2014) 2344–2351.
[24] J.E. Grebel, J.J. Pignatello, W.A. Mitch, Effect of halide ions and carbonates on organic contaminant degradation by hydroxyl radical-based advanced oxidation processes in saline waters, Environ. Sci. Technol. 44 (2010) 6822–6828.
[25] P.L. Altman, D.S. Dittmer, Blood and other body fluids, in: D.S. Dittmer (Ed.), Federation of American Societies for Experimental Biology, Washington, D.C, 1961.
[26] K. Hasegawa, P. Neta, Rate constants and mechanisms of reaction of Cl_2^- radicals, J. Phys. Chem. 82 (1978) 854–857.
[27] X. Shen, J. Lind, G. Merenyi, One-electron oxidation of indoles and acid-base properties of the indolyl radicals, J. Phys. Chem. 91 (1987) 4403–4406.
[28] J.Y. Liang, W.N. Lipscomb, Binding of substrate CO_2 to the active site of human carbonic anhydrase II: a molecular dynamics study, Proc. Natl. Acad. Sci. U.S.A. 87 (1990) 3675–3679.
[29] I. Fita, M.G. Rossmann, The active center of catalase, J. Mol. Biol. 185 (1985) 21–37.